

See discussions, stats, and author profiles for this publication at: <https://www.researchgate.net/publication/263549736>

Approximate First-Principles Anharmonic Calculations of Polyatomic Spectra Using MP2 and B3LYP Potentials: Comparisons with Experiment

ARTICLE *in* THE JOURNAL OF PHYSICAL CHEMISTRY A · JUNE 2014

Impact Factor: 2.69 · DOI: 10.1021/jp5060155 · Source: PubMed

CITATIONS

6

READS

57

3 AUTHORS, INCLUDING:



Tapta Kanchan Roy

Hebrew University of Jerusalem

16 PUBLICATIONS 131 CITATIONS

SEE PROFILE



Tucker Carrington

Queen's University

194 PUBLICATIONS 5,423 CITATIONS

SEE PROFILE

Approximate First-Principles Anharmonic Calculations of Polyatomic Spectra Using MP2 and B3LYP Potentials: Comparisons with Experiment

Tapta Kanchan Roy,[†] Tucker Carrington, Jr.,[‡] and R. Benny Gerber^{*,†,§,||}

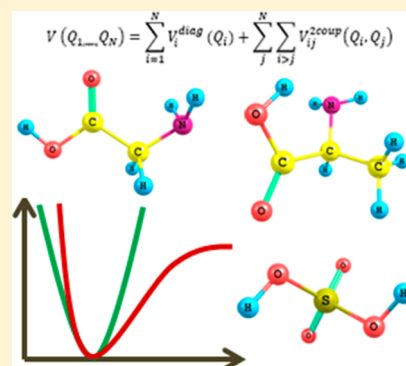
[†]Institute of Chemistry and The Fritz Haber Research Center, The Hebrew University, Jerusalem 91904, Israel

[‡]Chemistry Department, Queen's University, Kingston, Ontario K7L 3N6, Canada

[§]Department of Chemistry, University of Helsinki, P.O. Box 55, FIN-00014 Helsinki, Finland

^{||}Department of Chemistry, University of California, Irvine, California 92697, United States

ABSTRACT: Anharmonic vibrational spectroscopy calculations using MP2 and B3LYP computed potential surfaces are carried out for a series of molecules, and frequencies and intensities are compared with those from experiment. The vibrational self-consistent field with second-order perturbation correction (VSCF-PT2) is used in computing the spectra. The test calculations have been performed for the molecules HNO₃, C₂H₄, C₂H₄O, H₂SO₄, CH₃COOH, glycine, and alanine. Both MP2 and B3LYP give results in good accord with experimental frequencies, though, on the whole, MP2 gives very slightly better agreement. A statistical analysis of deviations in frequencies from experiment is carried out that gives interesting insights. The most probable percentage deviation from experimental frequencies is about −2% (to the red of the experiment) for B3LYP and +2% (to the blue of the experiment) for MP2. There is a higher probability for relatively large percentage deviations when B3LYP is used. The calculated intensities are also found to be in good accord with experiment, but the percentage deviations are much larger than those for frequencies. The results show that both MP2 and B3LYP potentials, used in VSCF-PT2 calculations, account well for anharmonic effects in the spectroscopy of molecules of the types considered.



1. INTRODUCTION

Vibrational spectroscopy is a powerful and widely used tool for characterizing the properties of molecular systems. In particular, it is an important tool for probing the quality of potential surfaces.^{1–5} Accurate computation of spectra generally requires many accurate ab initio points, an excellent fitting or interpolating function, good basis functions, and a means of calculating eigenvalues of the matrix representing the Hamiltonian in the basis.^{6–11} The question of which potential surfaces can be used to satisfactorily interpret experiment is of paramount importance. Our main objective of this paper is to explore how two extensively used quantum chemical methods B3LYP and MP2 describe the vibrational spectra in comparison with experiment and what their relative merits are. Previous comparisons between these methods were not systematic and were either limited to very few small molecules¹² or to some specific vibrational modes.¹³ Also, the important observable intensities given by different electronic structure methods were not tested satisfactorily. A few studies compared computed and experimental intensities for a few selected modes.^{13,14} Additionally, so far, no systematic analyses have been performed to generalize the error pattern given by these potentials when comparing with experiment. It is desirable to pursue some statistical analysis in order to get more general useful information as it is indeed important to have some prior

knowledge about the nature of deviations in calculated frequencies. What was done so far in this direction is not sufficient for those important and practical questions, and that motivates the present paper.

To calculate molecular vibrations, the harmonic oscillator (HO) approximation is often used, especially for large (e.g., biological) molecules.^{15–17} However, its accuracy is limited. An alternative for a better match with experiment is to use scaling factors. However, scaling of the HO^{18–20} is empirical and hence does not reflect on the quality of the potential. To achieve better accuracy, one needs to consider anharmonic approximations. For example, one can diagonalize a matrix representation of the Hamiltonian in a sufficiently large basis. The cost of such a calculation scales exponentially with the number of atoms in the molecule. We aim at molecules beyond the smallest ones; therefore, such rigorous vibrational methods cannot be used. Less expensive alternatives include perturbation theory^{21–25} and classical molecular dynamics (MD) simulation methods.²⁶ There are other approaches available in the literature.^{7,27–32}

Special Issue: Franco Gianturco Festschrift

Received: June 17, 2014

Revised: June 29, 2014

One such inexpensive and useful method is the vibrational self-consistent field (VSCF) approximation, which we have used here as a tool for testing the potentials. It was developed by Bowman,³³ Carney et al.,³⁴ Cohen et al.,³⁵ and Gerber and Ratner³⁶ and has been widely used.^{37–39} Initially, it was applied to small systems and later to large molecules such as proteins.^{40,41} Gerber and co-workers⁴² introduced a method that uses VSCF using the potentials given as points on a grid, obtained from electronic structure calculation. Several methods using ideas related to VSCF but including corrections or providing more accurate treatments were introduced. One such “corrected VSCF” algorithm, referred to as vibrational self-consistent field with second-order perturbation correction (VSCF-PT2^{43,44} or CC-VSCF) improved the VSCF algorithm by corrections from second-order perturbation theory. This method seemed to offer a useful balance between computational simplicity and accuracy. Later modifications made this method more suitable for large systems.^{45,46} Since then, a large number of applications have been derived by VSCF and VSCF-PT2. Bowman and co-workers have used VSCF + CI to study many molecules.^{27,47,48} Several other VSCF codes and various improved approaches also exist in the literature.^{49–67}

In this paper, we have tested two extensively used quantum chemical methods MP2 and B3LYP for the VSCF-PT2 calculations against experiment. To study the quality of these quantum chemical methods, we chose several types of molecules with 5–13 atoms and compared their frequencies with experiment. Also, we compared measured intensities with the computed where they were available. This was an additional demanding test. Next, we also computed and analyzed the distributions of deviations from experiments because this can give insights about the nature and range of errors that can be expected when using such quantum chemical methods. The main reason for choosing MP2 and B3LYP is that they are two high-level methods that can be used beyond the smallest molecules. Higher-level methods such as coupled cluster and MP4 are too costly for such calculations. In the spirit of this consideration, we will apply both methods with the cc-pVTZ basis, which by experience has given satisfactory results for relatively large molecules. In this study, we compute zero-point energies, fundamental frequencies, overtones and combination bands, and also intensities for a set of molecules for which these quantities are known experimentally.

In the next section, we briefly describe the VSCF-PT2 methodology and the approximations used in this work. Section 3 illustrates a few examples with error analysis, and in section 4, we discuss the accuracy of the MP2 and B3LYP potentials. Finally, the conclusions are given in section 5.

2. THEORY

In the VSCF method, coupling between different modes is treated by assuming that the full vibrational wave function can be factorized into single-mode wave functions. The single-mode wave functions are called modals. In practice, the factorization assumption is made for the normal modes. Equations for the wave functions and energy levels of the system are then derived on this basis. For each modal, a mean field potential that represents the average effects of the other modes is employed. All of the corresponding equations are solved numerically. The VSCF method and its extensions are discussed in detail in many previous publications. Details of the VSCF theory can be found in a recent review.⁶⁸

We can write the VSCF potential as a sum of one-mode (diagonal approximation) and pairwise coupling in terms of normal coordinate (Q)

$$V(Q_1, \dots, Q_N) = \sum_{i=1}^N V_i^{\text{diag}}(Q_i) + \sum_{j=1}^N \sum_{i>j} V_{ij}^{2\text{coup}}(Q_i, Q_j) \quad (1)$$

The potential represented in this form needs multidimensional grid point calculations, and the number of grid points increases rapidly with the dimensionality of the potential. If NG is the number of grid points along a normal mode and NV is the number of vibrational modes, then the number of total grid points (NP) is

$$\text{NP} = [\text{NV} \times \text{NG}] + \frac{[\text{NV}(\text{NV} - 1) \times \text{NG}^2]}{2} \quad (2)$$

To improve on VSCF further, vibrational levels are computed using second-order perturbation theory. This method is analogous to the Møller–Plesset method known in the context of electronic structure. The PT2 correction is described by the following equation

$$E_n^{\text{PT2}} = E_n^{\text{VSCF}} + \sum_{m \neq n} \frac{|\langle \prod_{j=1}^N \psi_j^{(n)}(Q_j) | \Delta V | \prod_{j=1}^N \psi_j^{(m)}(Q_j) \rangle|^2}{E_n^{(0)} - E_m^{(0)}} \quad (3)$$

where E_n^{PT2} is the correlation-corrected energy of the state n . The calculations here are carried out using GAMESS computational code.⁶⁹ Note that VSCF-PT2 can suffer from the problem of small denominators in cases of degeneracy, which may lead to the erroneous results. The simpler VSCF method, which is not a perturbative approach, does not suffer from this problem. VSCF-PT2 has been extended for dealing with such vibrational degeneracy and the corresponding resonances. This involves applying degenerate perturbation theory for correction beyond VSCF-PT2 (VSCF-DPT2).⁶¹ The relevant code is also included in recent GAMESS version.

Vibrational band intensities are evaluated (in km/mol) using values of the three components of the dipole moment calculated at the same points as the potential. We use an Eckart frame and compute integrated absorption coefficients for vibrational band intensities

$$I_i = \frac{8\pi^3 N_A}{3hc} \omega_i |\langle \psi_i^{(0)}(Q_i) | \vec{\mu}(Q_i) | \psi_i^{(m)}(Q_i) \rangle|^2 (n_0 - n_m) \quad (4)$$

This equation is written for the case where all of the initial population is in the vibrational ground state. The thermal effects on population are ignored in this study as $n_0 - n_m$, where n_0 and n_m are fractions of molecules in the initial and final states that are set equal to 1, corresponding to zero temperature.⁷⁰ $\psi_i^{(0)}$ and $\psi_i^{(m)}$ are VSCF-PT2 wave functions for the ground and excited vibrational states. The $\vec{\mu}$, as evaluated from electronic structure theory, is a function of the nuclear coordinates. If we use the equilibrium position as the origin, we can expand $\vec{\mu}$ in powers of normal coordinates. For fundamental and overtone transitions, it is a good approximation, at least for the low-lying states, to consider only $\vec{\mu}(0, \dots, Q_i, \dots, 0)$, which we denote by $\vec{\mu}(Q_i)$ for simplicity.^{13,71} The computed quantity of eq 4 corresponds to the experimental intensity. For combination

excitations of modes i and j (ignoring the population effect as stated above), we use

$$I_i = \frac{8\pi^3 N_A \omega_{ij}}{3hc} \times |\langle \psi_i^{(0)}(Q_i) \psi_j^{(0)}(Q_j) | \bar{u}(Q_i, Q_j) | \psi_i^{(m)}(Q_i) \psi_j^{(n)}(Q_j) \rangle|^2 \quad (5)$$

where m and n are the excitation levels for modes i and j and $\bar{u}(Q_i, Q_j)$ is a two-mode coordinate approximation to the dipole.

3. RESULTS

We have examined the MP2 and B3LYP potentials with available experimental values for a series of various small to medium sized molecules: HNO_3 , C_2H_4 , $\text{C}_2\text{H}_4\text{O}$, H_2SO_4 , CH_3COOH , glycine, and alanine. The reason to choose such systems is that our interest is largely in the molecules for which very accurate methods such as couple cluster are inapplicable for anharmonic calculations. Consequently, B3LYP and MP2 methods are manifested as the practical choices. It is already known that the final calculated spectra are also dependent on the basis, used and hence, to get better accuracy, we have systematically used correlation-consistent Dunning type triple- ξ (cc-pVTZ) basis sets⁷² for all of the systems.

A. HNO_3 . Nitric acid is a species of considerable importance in atmospheric chemistry, with nine vibrational modes. A large amount of experimental data is available for this molecule. Table 1 presents all of the fundamentals, selected overtones,

Table 1. Fundamentals, Overtones, and Combination Bands (cm^{-1}) of HNO_3 Calculated by VSCF-PT2^a versus Experiment

| mode | B3LYP | | MP2 | | exp ^b |
|--|-------|----------|-------|----------|------------------|
| | HO | VSCF-PT2 | HO | VSCF-PT2 | |
| ν_1 (OH str.) | 3720 | 3497 | 3750 | 3547 | 3550 |
| ν_2 (NO_2 asy. str.) | 1763 | 1713 | 1873 | 1847 | 1710 |
| ν_3 (NO_2 sym. str.) | 1351 | 1316 | 1350 | 1269 | 1326 |
| ν_4 (NOH bend) | 1324 | 1253 | 1334 | 1310 | 1304 |
| ν_5 (NO_2 deformation) | 904 | 886 | 909 | 887 | 879 |
| ν_6 (ONO_2 out of plane) | 786 | 774 | 782 | 772 | 763 |
| ν_7 (NO stretch) | 650 | 635 | 672 | 656 | 647 |
| ν_8 (ONO bend) | 588 | 568 | 593 | 574 | 580 |
| ν_9 (NOH torsion) | 499 | 402 | 497 | 407 | 458 |
| $2\nu_1$ | 7441 | 6857 | 7501 | 6946 | 6944 |
| $3\nu_1$ | 11161 | 10096 | 11251 | 10225 | 10173 |
| $4\nu_1$ | 14881 | 13323 | 15002 | 13482 | 13250 |
| $3\nu_1 + \nu_9$ | 11660 | 10687 | 11748 | 10856 | 10616 |
| $3\nu_1 + \nu_4$ | 12485 | 11299 | 12585 | 11547 | 11325 |

^aUsing 16 grid points per normal mode. ^bReference 73 and references therein.

and combination bands. It can be seen that the overall agreement between experiment and VSCF-PT2 is good and considerably more accurate than the HO values. However, the MP2 potential largely overestimates the NO_2 asymmetric stretching (ν_2) and underestimates the NO_2 symmetric stretching (ν_3). B3LYP underestimates the NOH bend (ν_4), while the NOH torsional motion (ν_9) is underestimated by both potentials. For other modes, both potentials result in good accuracy. B3LYP and MP2 give overtones and combination

bands with acceptable accuracy, though the errors are higher than the fundamental bands.

B. C_2H_4 . Ethylene is an important species in environmental chemistry, with 12 vibrational modes. In Table 2, the calculated

Table 2. Fundamentals and Combination Bands (cm^{-1}) of C_2H_4 Calculated by VSCF-PT2^a versus Experiment

| mode | B3LYP | | MP2 | | exp ^b |
|------------------------------------|-------|----------|------|----------|------------------|
| | HO | VSCF-PT2 | HO | VSCF-PT2 | |
| ν_1 (CH_2 asy. str.) | 3220 | 3078 | 3294 | 3154 | 3106 |
| ν_2 (CH_2 asy. str.) | 3191 | 3048 | 3268 | 3126 | 3103 |
| ν_3 (CH_2 sym. str.) | 3136 | 2993 | 3197 | 3051 | 3026 |
| ν_4 (CH_2 sym. str.) | 3123 | 2997 | 3179 | 3054 | 2989 |
| ν_5 (CC str.) | 1689 | 1660 | 1684 | 1644 | 1623 |
| ν_6 (CH_2 scis.) | 1473 | 1452 | 1485 | 1455 | 1444 |
| ν_7 (CH_2 scis.) | 1380 | 1358 | 1384 | 1358 | 1342 |
| ν_8 (CH_2 rock) | 1245 | 1231 | 1247 | 1232 | 1236 |
| ν_9 (CH_2 twist) | 1067 | 1049 | 1076 | 1058 | 1023 |
| ν_{10} (CH_2 wag) | 982 | 971 | 983 | 971 | 949 |
| ν_{11} (CH_2 wag) | 977 | 969 | 960 | 949 | 943 |
| ν_{12} (CH_2 rock) | 831 | 844 | 828 | 834 | 826 |
| $\nu_8 + \nu_{12}$ | 2075 | 2086 | 2074 | 2077 | 2048 |
| $\nu_{10} + \nu_{11}$ | 1959 | 1965 | 1943 | 1945 | 1889 |

^aUsing 16 grid points per normal mode. ^bShimanouchi, T. *Tables of Molecular Vibrational Frequencies Consolidated Volume I*; National Bureau of Standards: Gaithersburg, MD, 1972, pp 1–160.

frequencies obtained by VSCF-PT2 are given. Here again, MP2 and B3LYP show considerable accuracy. As is true for most of the molecules, the MP2 potential systematically overestimates (except ν_8) the experimental values, whereas B3LYP underestimates (except ν_4) the high-frequency range and overestimates (except ν_8) the mid-IR and low-frequency ranges. For some of the C–H stretches, MP2 is better, and for others, B3LYP is better. Overall, agreement is good for this molecule.

C. $\text{C}_2\text{H}_4\text{O}$. Next, we considered the simplest epoxide with seven atoms, ethylene oxide. In Table 3, we present the fundamentals of ethylene oxide. Again, like ethylene, MP2

Table 3. Fundamental Bands (cm^{-1}) of $\text{C}_2\text{H}_4\text{O}$ Calculated by VSCF-PT2^a versus Experiment

| mode | B3LYP | | MP2 | | exp ^b |
|------------------------------------|-------|----------|------|----------|------------------|
| | HO | VSCF-PT2 | HO | VSCF-PT2 | |
| ν_1 (CH_2 asy. str.) | 3173 | 3023 | 3261 | 3113 | 3065 |
| ν_2 (CH_2 asy. str.) | 3157 | 3005 | 3246 | 3097 | 3065 |
| ν_3 (CH_2 sym. str.) | 3086 | 2947 | 3156 | 3057 | 3024 |
| ν_4 (CH_2 sym. str.) | 3079 | 2947 | 3150 | 3018 | 2978 |
| ν_5 (CH_2 scis.) | 1540 | 1501 | 1556 | 1515 | 1498 |
| ν_6 (CH_2 scis.) | 1506 | 1475 | 1521 | 1489 | 1470 |
| ν_7 (ring str.) | 1299 | 1273 | 1314 | 1285 | 1270 |
| ν_8 (CH_2 rock) | 1175 | 1162 | 1184 | 1171 | 1150 |
| ν_9 (CH_2 twist) | 1170 | 1155 | 1179 | 1163 | 1147 |
| ν_{10} (CH_2 wag) | 1154 | 1145 | 1159 | 1149 | 1159 |
| ν_{11} (CH_2 twist) | 1148 | 1133 | 1156 | 1138 | 1120 |
| ν_{12} (CH_2 twist) | 1045 | 1031 | 1058 | 1044 | 1020 |
| ν_{13} (ring str.) | 887 | 869 | 909 | 887 | 877 |
| ν_{14} (CO str.) | 842 | 818 | 858 | 831 | 822 |
| ν_{15} (CH_2 rock) | 818 | 818 | 823 | 822 | 808 |

^aUsing 12 grid points per normal mode. ^bReference 74 and references therein.

Table 4. Fundamentals and Combination Bands (cm⁻¹) of H₂SO₄ by VSCF-PT2^a versus Experiment

| mode | B3LYP | | MP2 | | exp ^b |
|--|-------|----------|------|----------|------------------|
| | HO | VSCF-PT2 | HO | VSCF-PT2 | |
| ν_1 (OH sym. str.) | 3762 | 3504 | 3801 | 3543 | 3609 |
| ν_2 (OH asy. str.) | 3758 | 3421 | 3796 | 3463 | |
| ν_3 (S=O ₂ asy. str.) | 1474 | 1448 | 1518 | 1493 | 1465 |
| ν_4 (S=O ₂ sym. str.) | 1224 | 1205 | 1260 | 1244 | 1220 |
| ν_5 (SOH asy. bend) | 1162 | 1102 | 1179 | 1114 | 1157 |
| ν_6 (SOH sym. bend) | 1145 | 1068 | 1161 | 1083 | 1138 |
| ν_7 (S(OH) ₂ asy. str.) | 868 | 852 | 903 | 882 | 891 |
| ν_8 (S(OH) ₂ sym. str.) | 814 | 799 | 849 | 833 | 834 |
| ν_9 (O-S=O rock) | 551 | 546 | 563 | 558 | 568 |
| ν_{10} (S=O ₂ bend) | 540 | 550 | 552 | 560 | 550 |
| ν_{11} (S=O ₂ wag) | 495 | 459 | 504 | 469 | |
| ν_{12}^c (O-S=O bend) | 431 | 431 | 447 | 447 | |
| ν_{13} (OH asy. torsion) | 369 | 365 | 383 | 374 | 281 |
| ν_{14} (O-S=O twist) | 308 | 293 | 337 | 319 | |
| ν_{15}^c (OH sym. torsion) | 223 | 223 | 249 | 249 | 216 |
| $\nu_1 + \nu_5$ | 4924 | 4536 | 4980 | 4620 | 4739 |
| $\nu_2 + \nu_{15}$ | 3981 | 3689 | 4046 | 3768 | 3825 |

^aUsing 12 grid points per normal mode. ^bReference 75. ^cVSCF-PT2 fails for those transitions, and hence, HO values are kept.

Table 5. Fundamental Bands (cm⁻¹) of CH₃COOH Calculated by VSCF-PT2^a versus Experiment

| mode | B3LYP | | MP2 | | exp ^b |
|--------------------------------------|-------|----------|------|----------|------------------|
| | HO | VSCF-PT2 | HO | VSCF-PT2 | |
| ν_1 (OH str.) | 3738 | 3522 | 3773 | 3555 | 3583 |
| ν_2 (CH ₃ d-str.) | 3158 | 2915 | 3230 | 2975 | 3051 |
| ν_3 (CH ₃ d-str.) | 3107 | 2848 | 3187 | 2920 | 2996 |
| ν_4 (CH ₃ s-str.) | 3050 | 2874 | 3104 | 2913 | 2944 |
| ν_5 (C=O str.) | 1825 | 1775 | 1833 | 1785 | 1788 |
| ν_6 (CH ₃ d-deform) | 1482 | 1456 | 1497 | 1477 | 1430 |
| ν_7 (CH ₃ d-deform) | 1473 | 1449 | 1489 | 1468 | 1430 |
| ν_8 (CH ₃ s-deform) | 1410 | 1358 | 1423 | 1373 | 1382 |
| ν_9 (OH bend) | 1342 | 1298 | 1350 | 1309 | 1264 |
| ν_{10} (CC str.) | 1206 | 1172 | 1211 | 1181 | 1182 |
| ν_{11} (CH ₃ rock) | 1073 | 1057 | 1074 | 1060 | 1048 |
| ν_{12} (CH ₃ rock) | 1005 | 988 | 1006 | 999 | 989 |
| ν_{13} (CC str.) | 859 | 840 | 878 | 858 | 847 |
| ν_{14} (OCO deform) | 672 | 773 | 671 | 772 | 657 |
| ν_{15} (C=O oop bend) | 585 | 575 | 585 | 575 | 642 |
| ν_{16} (CCO deform) | 551 | 537 | 553 | 529 | 581 |
| ν_{17} (C-O torsion) | 426 | 426 | 423 | 431 | 534 |
| ν_{18} (CH ₃ torsion) | 72 | 119 | 76 | 125 | |

^aUsing eight grid points per normal mode. ^bShimanouchi, T. *Tables of Molecular Vibrational Frequencies Consolidated Volume I*; National Bureau of Standards: Gaithersburg, MD, 1972, pp 1–160.

systematically overestimates (except ν_{10}) the experimental values throughout the frequency range, whereas B3LYP systematically underestimates the high-frequency range and overestimates (except ν_{10} , ν_{13} , ν_{14}) the mid-IR and lower-frequency ranges. Here again, for some of the C–H stretching frequencies, MP2 is better, and for some of them, B3LYP is better. However, the magnitude of errors for C–H stretches given by MP2 is less than B3LYP. Overall, for most of the cases, the agreement between the experimental and calculated values is good.

D. H₂SO₄. H₂SO₄ is a common acid that is important in atmospheric chemistry. Its vibrational spectra have been studied experimentally.^{76,77} As can be seen in Table 4, both the MP2 and B3LYP have generally reasonable agreement with experiment, with a few exceptions. For combination bands, MP2 has

smaller errors than B3LYP. However, the overall error in this system is higher than that in the other systems that we have studied. That may be due to the inadequacy in the basis for heavy atoms like sulfur.

E. CH₃COOH. Next, we calculated an 18 vibrational mode molecule, acetic acid. In Table 5, we show the comparison of the calculated and experimental results for the fundamentals. It can be seen that both methods underestimate the experimental values in the high-frequency range. Overall, the MP2 potential is again superior to the B3LYP. In the mid-IR and lower-frequency range, both methods result in errors on both sides of the experimental values, however, with reasonable accuracy.

F. Glycine. Finally, we have tested the B3LYP and MP2 potentials for two amino acids, glycine and alanine. Glycine, the smallest amino acid, has been the topic of several theoretical

and experimental spectroscopic studies.^{66,78–81} This flexible 24 vibrational mode system has three low-energy conformers. In Table 6, we show the comparison among calculated and

Table 6. Fundamental Bands (cm^{-1}) of Glycine Calculated by VSCF-PT2^a versus Experiment

| mode | B3LYP | | MP2 | | exp ^b |
|---|-------|----------|------|----------|------------------|
| | HO | VSCF-PT2 | HO | VSCF-PT2 | |
| ν_1 (OH str.) | 3735 | 3501 | 3770 | 3542 | 3560 |
| ν_2 (NH ₂ asy. str.) | 3562 | 3255 | 3623 | 3321 | 3410 |
| ν_3 (NH ₂ sym. str.) | 3495 | 3192 | 3538 | 3299 | |
| ν_4 (CH ₂ asy. str.) | 3064 | 2856 | 3148 | 2925 | |
| ν_5 (CH ₂ sym. str.) | 3037 | 2864 | 3100 | 2938 | 2958 |
| ν_6 (C=O str.) | 1819 | 1767 | 1827 | 1776 | 1779 |
| ν_7 (NHN bend) | 1675 | 1620 | 1677 | 1623 | 1630 |
| ν_8 (HCH bend) | 1463 | 1418 | 1473 | 1431 | 1429 |
| ν_9 (C–O(H) str.) | 1399 | 1348 | 1421 | 1373 | 1373 |
| ν_{10} (CCN bend) | 1385 | 1340 | 1399 | 1349 | |
| ν_{11} (NCH ₂ bend) | 1311 | 1259 | 1317 | 1270 | |
| ν_{12} (CCN oop bend) | 1188 | 1157 | 1195 | 1161 | |
| ν_{13} (CN str.) | 1159 | 1135 | 1181 | 1152 | 1136 |
| ν_{14} (CO ₂ bend) | 1122 | 1079 | 1142 | 1100 | 1101 |
| ν_{15} (CNH ₂ bend) | 925 | 925 | 956 | 951 | 907 |
| ν_{16} (CCO oop bend) | 911 | 912 | 925 | 919 | 883 |
| ν_{17} (CO ₂ –C str.) | 821 | 800 | 843 | 827 | 801 |
| ν_{18} (CO ₂ oopb) | 654 | 741 | 656 | 743 | 619 |
| ν_{19} (NCCO(H) shear) | 638 | 632 | 639 | 634 | |
| ν_{20} (OCO(H) tors) | 504 | 492 | 515 | 483 | 500 |
| ν_{21} (NCCO(H) shear) | 463 | 457 | 468 | 463 | 463 |
| ν_{22} (NCCO shear) | 262 | 268 | 260 | 272 | |
| ν_{23}^c (NH ₂ group tors) | 219 | 219 | 218 | 218 | |
| ν_{24}^c (NCCO(H) tors) | 56 | 56 | 65 | 65 | |

^aUsing eight grid points per normal mode. ^bReference 66 and references therein. ^cVSCF-PT2 fails for this transition, and hence, HO values are kept.

experimental results for the fundamentals of the lowest-energy conformer of glycine.⁶⁶ It is found that the ν_5 in B3LYP and ν_{18} in both methods have large errors. Other modes are quite satisfactory compared to the experiment. In this case, the high-frequency modes are underestimated by both methods, and the mid-IR and low-frequency ranges are overestimated, for most cases with reasonable accuracy.

G. Alanine. The largest system that we studied is alanine, with 33 vibrational modes. Alanine also has three low-energy conformers, and we chose the second lowest structure as it has the largest number of available experimental frequencies.⁸² As can be seen from Table 7, except ν_5 (asy. CH stretching) and ν_9 (HNH bend), all other vibrational modes show impressive accuracy for the MP2 potential. The errors are distributed on both sides of the experimental values. The B3LYP potential shows higher errors than MP2 in particular for ν_4 , ν_5 , ν_{15} , and ν_{20} , and most of the vibrational modes are underestimated.

H. IR Absorption Intensity. IR absorption intensities are important observables in vibrational spectroscopy. Their computed values are often in much less satisfactory accord with experiment than frequencies. Intensities depend directly on the vibrational wave functions of the initial and final states of the transition. Therefore, the intensity provides additional information for the accuracy of a given PES. In Table 8, we show the relative intensities of ethylene oxide obtained from

Table 7. Fundamental Bands (cm^{-1}) of Alanine Calculated by VSCF-PT2^a versus Experiment

| mode | B3LYP | | MP2 | | exp ^b |
|--|-------|----------|------|----------|------------------|
| | HO | VSCF-PT2 | HO | VSCF-PT2 | |
| ν_1 (NH ₂ asy. str.) | 3589 | 3240 | 3635 | 3308 | |
| ν_2 (NH ₂ sym. str.) | 3510 | 3411 | 3541 | 3353 | |
| ν_3 (OH str.) | 3467 | 3172 | 3495 | 3201 | 3193 |
| ν_4 (CH ₃ asy. str.) | 3126 | 2893 | 3191 | 2971 | 2982 |
| ν_5 (CH ₃ asy. str.) | 3089 | 2798 | 3163 | 2885 | 2943 |
| ν_6 (CH str.) | 3033 | 2873 | 3103 | 2940 | 2914 |
| ν_7 (CH ₃ sym. str.) | 3028 | 2887 | 3076 | 2900 | 2885 |
| ν_8 (C=O str.) | 1844 | 1788 | 1847 | 1793 | 1792 |
| ν_9 (HNH bend) | 1664 | 1591 | 1655 | 1597 | 1642 |
| ν_{10} (HCH bend (Me)) | 1504 | 1459 | 1516 | 1476 | 1460 |
| ν_{11} (HCH bend (Me)) | 1499 | 1456 | 1512 | 1473 | 1457 |
| ν_{12} (C–Me str., CH ₃ bend) | 1419 | 1356 | 1433 | 1373 | 1368 |
| ν_{13} (C–O(H) str.) | 1408 | 1370 | 1408 | 1370 | 1376 |
| ν_{14} (CN str.) | 1360 | 1312 | 1367 | 1319 | |
| ν_{15} (MeCN bend) | 1328 | 1285 | 1348 | 1303 | 1336 |
| ν_{16} (MeCN oop bend) | 1275 | 1226 | 1284 | 1242 | |
| ν_{17} (CO ₂ sym. str.) | 1205 | 1163 | 1225 | 1187 | 1211 |
| ν_{18} (CN str.) | 1125 | 1094 | 1151 | 1111 | |
| ν_{19} (CCC bend) | 1058 | 1038 | 1067 | 1048 | |
| ν_{20} (C–Me str.) | 1019 | 983 | 1031 | 1010 | 1037 |
| ν_{21} (MeCN bend) | 941 | 939 | 963 | 958 | |
| ν_{22} (CN str.) | 871 | 778 | 895 | 809 | |
| ν_{23} (OCO(H) tors) | 849 | 807 | 865 | 828 | 812 |
| ν_{24} (HO ₂ C–CH str.) | 799 | 799 | 816 | 813 | 786 |
| ν_{25} (CO ₂ oop bend) | 744 | 734 | 749 | 738 | |
| ν_{26} (CCC oop bend) | 635 | 624 | 646 | 638 | 625 |
| ν_{27} (CO ₂ bend) | 530 | 521 | 535 | 529 | 493 |
| ν_{28} (NCCO tor) | 393 | 386 | 391 | 376 | |
| ν_{29} (NCCO(H) shear) | 343 | 340 | 346 | 349 | |
| ν_{30} (NH ₂ group tors) | 279 | 365 | 297 | 410 | |
| ν_{31} (CH ₃ group tors) | 266 | 381 | 260 | 339 | |
| ν_{32} (MeCCO ₂ tors) | 245 | 216 | 242 | 221 | |
| ν_{33} (CO ₂ group tors) | 73 | 89 | 79 | 93 | |

^aUsing eight grid points per normal mode. ^bReference 66 and references therein.

the HO and VSCF-PT2 algorithm for both the MP2 and B3LYP potentials and compare them with experimental values. For fundamentals and overtones, we include only a single-coordinate term in the dipole operator. For combination bands, we use a two-mode coordinate approximation for the dipole operator. It is found that VSCF-PT2 intensities using both the potentials result in better agreement with experiment than the HO values. For most of the cases, the VSCF-PT2 correction over HO shifts toward the experimental values. Once again, as we have seen in frequency tables that the MP2 potential gives better intensities than the B3LYP potential.

I. Error Analysis. To assess the errors in the calculated frequencies given by the MP2 and B3LYP potentials, we evaluated the mean absolute percentage error (MAPE) for the fundamentals of the molecules stated above. We use the equation

Table 8. Comparison of the Relative Intensities of C₂H₄O Calculated by VSCF-PT2 versus Experiment (km/mol)^a

| mode | B3LYP | | MP2 | | exp ^b |
|------------|--------|----------|-------|----------|------------------|
| | HO | VSCF-PT2 | HO | VSCF-PT2 | |
| ν_1 | 0.716 | 0.774 | 0.464 | 0.507 | 0.567 |
| ν_2 | 0.002 | 0.000 | 0.003 | 0.000 | 0.000 |
| ν_3 | 0.264 | 0.248 | 0.227 | 0.206 | 0.094 |
| ν_4 | 0.631 | 0.656 | 0.447 | 0.460 | 0.693 |
| ν_5 | 0.049 | 0.038 | 0.037 | 0.026 | 0.016 |
| ν_6 | 0.002 | 0.000 | 0.002 | 0.000 | 0.005 |
| ν_7 | 0.201 | 0.218 | 0.162 | 0.176 | 0.206 |
| ν_8 | 0.003 | 0.000 | 0.003 | 0.000 | 0.000 |
| ν_9 | 0.043 | 0.052 | 0.047 | 0.056 | |
| ν_{10} | 0.025 | 0.053 | 0.029 | 0.023 | |
| ν_{11} | 0.002 | 0.000 | 0.013 | 0.007 | |
| ν_{12} | 0.001 | 0.000 | 0.001 | 0.000 | 0.000 |
| ν_{13} | 1.000 | 1.000 | 1.000 | 1.000 | 1.000 |
| ν_{14} | 0.172 | 0.018 | 0.136 | 0.145 | 0.134 |
| ν_{15} | 0.0032 | 0.000 | 0.004 | 0.0002 | 0.003 |

^aNormalized with respect to the maximum intensity (ν_{13}). ^bReference 83 and references therein.

$$\text{MAPE} = \frac{100}{n} \sum_{i=1}^n \left| \frac{\nu_{\text{ref}}^i - \nu_{\text{calc}}^i}{\nu_{\text{ref}}^i} \right| \quad (16)$$

where n is the number of vibrational modes. Here, ν_{ref} are the experimental values, and ν_{calc} are the calculated values. The ν_{calc} are values from either HO or VSCF-PT2, for both quantum chemistry methods. The MAPEs for all of the cases are shown in Table 9. It is clearly seen that MP2 consistently improves

Table 9. Comparison of the MAPE in Frequencies with Experiment (eq 16)

| molecule | B3LYP | | MP2 | |
|---------------------------------|---------------|---------------------|---------------|---------------------|
| | HO versus exp | VSCF-PT2 versus exp | HO versus exp | VSCF-PT2 versus exp |
| HNO ₃ | 3.11 | 2.75 | 4.42 | 3.17 |
| C ₂ H ₄ | 3.10 | 1.52 | 3.73 | 1.35 |
| C ₂ H ₄ O | 2.26 | 1.03 | 3.72 | 1.38 |
| H ₂ SO ₄ | 4.60 | 5.62 | 6.56 | 6.12 |
| CH ₃ COOH | 4.47 | 4.72 | 5.35 | 4.52 |
| Glycine | 2.62 | 2.89 | 4.15 | 2.76 |
| Alanine | 3.43 | 2.00 | 4.47 | 1.76 |

MAPEs for VSCF-PT2 better than those for HO. On the contrary, B3LYP does not improve MAPEs for many cases. We note that the VSCF-PT2 corrections by B3LYP over HO are

relatively more erroneous for some of the transition. Those large deviations lead to MAPEs that are larger than their HO counterparts. Additionally, B3LYP gives more such large deviations than MP2, which makes it somewhat less accurate than MP2. As a further analysis of errors in the calculated frequencies, we plot two histograms to assess the statistical distribution of the percentage error by B3LYP and MP2 with experiment. We have included the fundamental frequencies of all of the molecules tested here with an error range of -5 to 10% . As can be seen from Figure 1, the accuracy of both methods is roughly the same with an error range of $\pm 2\%$. A sharp peak for the MP2 potential at -2 to -1% shows that the majority of the errors are localized in this range. On the other hand, the B3LYP errors are more distributed on both sides of the experimental values, and the majority of the errors are located between 0 and 2% . Overall, the most probable transition by MP2 is blue-shifted with respect to experiment, and for B3LYP, it is red-shifted. It shows that the MP2 potential is stiffer and binds stronger, whereas B3LYP leads to a softer potential. It is also found that for the high-frequency range, the MP2 potential overestimates most of the experimental values, and B3LYP underestimates them. In the low-frequency range, both potentials generally overestimate the frequencies, where MP2 overestimates more frequencies than B3LYP. That finally makes MP2 blue-shifted, while B3LYP is red-shifted. Such different natures of the error pattern given by the two potentials should provide ideas about the expected accuracy of calculations with these methods.

4. DISCUSSION

From the series of molecules we have studied to test the accuracy and performance of the MP2 and B3LYP potentials against experiment, it was found that MP2, in general, gives somewhat better accuracy than B3LYP throughout the frequency range. B3LYP has comparable accuracy to MP2 for the lower-frequency range but underestimates the higher-frequency range more in particular for hydrogenic stretches. For example, B3LYP underestimates all of the C–H stretching frequencies of ethylene (except ν_4), ethylene oxide, and acetic acid. In particular for acetic acid, the errors are substantial. On the other hand, MP2 systematically overestimates these frequencies for ethylene and ethylene oxide but underestimates them for acetic acid. For most of the cases, the magnitude of errors for the stretching frequencies in MP2 is less than that in B3LYP. Similarly, we found that one of the C–H stretches (ν_5) in alanine shows a larger deviation in B3LYP than in MP2. It seems that the vibrations of the $-\text{CH}_3$ group are not well described by these two potentials, B3LYP in particular. Roie et al.¹³ found that for some small organic molecules, B3LYP

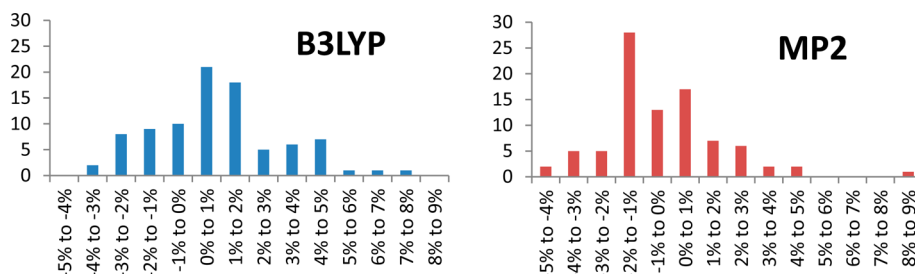


Figure 1. Histograms of the % error distributions by B3LYP (blue) and MP2 (red) against experiment for all of the vibrational modes. The y axis corresponds to the number of vibrations that belong to the error range given in the x axis.

shows somewhat better accuracy than MP2 for C–H stretching using the cc-pVDZ basis. Our systematic study using larger bases shows that this is not the case, in general. The calculated intensities by both potentials are comparable with experiment and generally better than HO, though the correction is not dramatic. Here again, MP2 results in slightly better agreement than B3LYP.

The error analyses show that in MP2, the probability of getting a large error (magnitude > 2%) is less than that in B3LYP, that is, the errors are more localized. In general, MP2 overestimates a larger number of frequencies, while B3LYP underestimates, and that finally results in MP2 being blue-shifted and B3LYP being red-shifted with respect to experiment.

It is noted that the MP2 and B3LYP methods produce very similar anharmonic corrections ($\nu_{\text{HO}} - \nu_{\text{Anham}}$), which shows that both methods estimate the anharmonicity to the same level of accuracy. For example, the anharmonic corrections for the first four high-frequency modes of ethylene are 142, 143, 143, and 126 cm^{-1} and 140, 142, 146, and 125 cm^{-1} using B3LYP and MP2 potentials, respectively. The same trend is also observed for the mid-IR and low-frequency ranges and also for other systems. That implies that the final accuracy also depends on the quality of the HO values given by a particular method. To check the anharmonic correction in a more systematic way for some physical insight extracted from numerical calculation, we have examined the stepwise corrections due to VSCF-PT2 algorithm in each step for the C–H stretching frequencies of ethylene. We have found that for most of the cases, the intrinsic anharmonicity (diagonal approximation) increases the frequency values by a few tens of wavenumbers on top of the HO values. Next, the VSCF approximation brings down the values extensively toward the experimental values, and finally VSCF-PT2 generally further reduces the frequencies by a few tens of wavenumbers on top of the VSCF values for final results that are then close to the experimental values.

Within this direct VSCF-PT2 approximation, the number of grid points is another source of error. We have tested a few molecules with variable grid points and found that for rigid and semirigid molecules, 8–10 grid points per normal mode are sufficient, and for soft systems 12–16 grid points are necessary. For example, $\text{C}_2\text{H}_4\text{O}$ gives converged results for 12 grid points but not for 8 grid points. Note that the CPU time largely depends on the number of multidimensional grid points, and hence, one should choose it depending on the size and nature of the molecule of interest.

To this end, it is also important to comment on the VSCF-PT2 approximation with another common approach, the second-order perturbative correction on the harmonic vibrational levels (VPT2). We have performed VPT2 calculation for a subset of molecules that we have studied here using Barone's algorithm given in the Gaussian package.⁸⁴ We found that both approximations work equally well for most of the cases. The mean deviations for VPT2 from experiment are essentially of the same magnitude as those for VSCF-PT2. We found that when using B3LYP, both approximations work well, and the differences are small for most of the cases. For example, the mean % deviations due to B3LYP using VPT2 and VSCF-PT2 are the same (1.03%) for ethylene oxide, while for ethylene, these are 1.52 and 1.20%, respectively. However, for the H_2SO_4 molecule, VPT2 has a larger error (13.17%) in comparison to VSCF-PT2 (5.62%) due to the poor description of the lower vibrational modes. On the other hand, it seems that VPT2

using MP2 does slightly better on the average frequencies than VSCF-PT2. Overall, MP2 works marginally more consistently than B3LYP for VPT2 with fewer fluctuations in error, which is also the case of VSCF-PT2 calculations. Finally, it is found that for most of the cases both with B3LYP and with MP2, VPT2 gives comparable results to the VSCF-PT2 method. Further systematic study is needed in this direction.

We should also note that the potential in our VSCF-PT2 approximation is based on normal coordinates. It is found that for various cases, the normal coordinate representation is not sufficient to represent some soft vibrations such as torsional motion of $-\text{CH}_3$, where the couplings between the torsional modes and other normal modes are large. Several other coordinate systems have been explored and used successfully with higher accuracy.^{65,85–93} However, due to large cross terms in the kinetic energy operator, those methods have been applied only on some limited small systems. More studies are needed in this direction for other coordinate systems.

Finally, we show how two reliable first-principle-based methods can predict the anharmonic vibrational frequencies and intensities. The accuracy and error distribution given by these two potentials in comparison to the experimental data offer a choice for future calculations. Overall, this study offers the efficacy of computed spectra for a choice of potentials, which can help future analyses while comparing extensive computed data with experiment.

5. CONCLUDING REMARKS

In this contribution, we have assessed the performance, accuracy, and applicability of MP2 and B3LYP potentials for the VSCF-PT2 algorithm with applications for a set of molecules. It is found that both methods are satisfactory tools for computing the vibrational spectra in the present state-of-the-art methods, while MP2 seems on the whole somewhat more accurate. The intensities calculated with these two potentials are comparable and better than HO, and MP2 again comes out as a marginally better method than B3LYP. Statistical analysis revealed that the distribution pattern of errors of these two methods is different, and most of the errors are in the range of $\pm 2\%$. Overall, MP2 results in blue-shifted frequencies and B3LYP in red-shifted. Finally, the statistical analysis in order to characterize the deviation from experiment suggests that it can be useful in extracting conclusions from extensive test calculations. Finally, these two widely used standard algorithms B3LYP and MP2, which are viewed generally as approximately of the same level of accuracy, give a reasonable level of agreement with experiment, which would be useful in the future for the interpretation of vibrational spectroscopic data.

AUTHOR INFORMATION

Corresponding Author

*E-mail: benny@fh.huji.ac.il.

Notes

The authors declare no competing financial interest.

ACKNOWLEDGMENTS

T.K.R. thanks Dr. B. Brauer for fruitful discussion and Dr. V. Sarkar for helping during the preparation of this manuscript. We thank Research at the Hebrew University that was supported by resources of the Saaree K. and Louis P. Fiedler Chair in Chemistry (RBG). T.K.R. thanks the CSC-IT Center

for Science, Finland for the computational resources and the PBC post doctoral fellowship, Council of Higher Education, Israel. R.B.G. thanks the Academy of Finland for supporting in the framework of the FiDiPro program. T.C. thanks NSERC of Canada for financial support.

REFERENCES

- (1) Gerber, R. B.; Chaban, G. M.; Brauer, B.; Miller, Y. *Theory and applications of computational chemistry: The first 40 years*; Elsevier: Amsterdam, The Netherlands, 2005; Chapter 9, pp 165–193.
- (2) Pratt, D. W. High resolution spectroscopy in the gas phase: Even large molecules have well-defined shapes. *Annu. Rev. Phys. Chem.* **1998**, *49*, 481–530.
- (3) Chaban, G. M.; Jung, J. O.; Gerber, R. B. Anharmonic vibrational spectroscopy of hydrogen-bonded systems directly computed from ab initio potential surfaces: $(\text{H}_2\text{O})_n$, $n = 2, 3$; $\text{Cl}^-(\text{H}_2\text{O})_n$, $n = 1, 2$; $\text{H}^+(\text{H}_2\text{O})_n$, $n = 1, 2$; $\text{H}_2\text{O}-\text{CH}_3\text{OH}$. *J. Phys. Chem. A* **2000**, *104*, 2772–2779.
- (4) Brauer, B.; Gerber, R. B.; Kabeláč, M.; Hobza, P.; Bakker, J. M.; Riziq, A. G. A.; de Vries, M. S. Vibrational spectroscopy of the G...C base pair: Experiment, harmonic and anharmonic calculations, and the nature of the anharmonic couplings. *J. Phys. Chem. A* **2005**, *109*, 6974–6984.
- (5) Carbonniere, P.; Barone, V. Performances of different density functionals in the computation of vibrational spectra beyond the harmonic approximation. *Chem. Phys. Lett.* **2004**, *399*, 226–229.
- (6) Vendrell, O.; Brill, M.; Gatti, F.; Lauvergnat, D.; Mayer, H.-D. Full dimensional (15-dimensional) quantum-dynamical simulation of the protonated water-dimer III: Mixed Jacobi-valence parametrization and benchmark results for the zero point energy, vibrationally excited states, and infrared spectrum. *J. Chem. Phys.* **2009**, *130*, 234305–234313.
- (7) Wang, X.-G.; Carrington, T., Jr. Vibrational energy levels of CH_3^+ . *J. Chem. Phys.* **2008**, *129*, 234102–234113.
- (8) Carter, S.; Sharma, A. R.; Bowman, J. M.; Rosmus, P.; Tarroni, R. Calculations of rovibrational energies and dipole transition intensities for polyatomic molecules using MULTIMODE. *J. Chem. Phys.* **2009**, *131*, 224106–224115.
- (9) Carter, S.; Sharma, A. R.; Bowman, J. M. Multimode calculations of rovibrational energies and dipole transition intensities for polyatomic molecules with torsional motion: Application to H_2O_2 . *J. Chem. Phys.* **2011**, *135*, 014308–014310.
- (10) Avila, G.; Carrington, T., Jr. Using a pruned basis, a non-product quadrature grid, and the exact Watson normal-coordinate kinetic energy operator to solve the vibrational Schrödinger equation for C_2H_4 . *J. Chem. Phys.* **2011**, *135*, 064101–064112.
- (11) Tremblay, J. C.; Carrington, T., Jr. Calculating vibrational energies and wave functions of vinylidene using a contracted basis with a locally reorthogonalized coupled two-term Lanczos eigensolver. *J. Chem. Phys.* **2006**, *125*, 094311–094312.
- (12) Chaban, G. M.; Gerber, R. B. Anharmonic vibrational spectroscopy calculations with electronic structure potentials: Comparison of MP2 and DFT for organic molecules. *Theor. Chem. Acc.* **2008**, *120*, 273–279.
- (13) Knaanie, R.; Sebek, J.; Kalinowski, J.; Gerber, R. B. Hybrid MP2/MP4 potential surfaces in VSCF calculations of IR spectra: Applications for organic molecules. *Spectrochim. Acta, Part A* **2014**, *119*, 2–11.
- (14) Sebek, J.; Pele, L.; Potma, E. O.; Gerber, R. B. Raman spectra of long chain hydrocarbons: Anharmonic calculations, experiment and implications for imaging of biomembranes. *Phys. Chem. Chem. Phys.* **2011**, *13*, 12724–12733.
- (15) Mirkin, N. G.; Krimm, S. Ab initio vibrational analysis of hydrogen-bonded *trans*- and *cis*-*N*-methylacetamide. *J. Am. Chem. Soc.* **1991**, *113*, 9742–9747.
- (16) Csaszar, A. G. On the structures of free glycine and α -alanine. *J. Mol. Struct.* **1995**, *346*, 141–152.
- (17) Csaszar, A. G. Conformers of gaseous α -alanine. *J. Phys. Chem.* **1996**, *100*, 3541–3551.
- (18) Scott, A. P.; Radom, L. Harmonic vibrational frequencies: An evaluation of Hartree–Fock, Møller–Plesset, quadratic configuration interaction, density functional theory and semiempirical scale factors. *J. Phys. Chem.* **1996**, *100*, 16502–16513.
- (19) Halls, M. D.; Velkovski, J.; Schlegel, H. B. Harmonic frequency scaling factors for Hartree–Fock, S-VWN, B-LYP, B3-LYP, B3-PW91 and MP2 with the Sadlej pVTZ electric property basis set. *Theor. Chem. Acc.* **2001**, *105*, 413–421.
- (20) Merrick, J. P.; Moran, D.; Radom, L. An evaluation of harmonic vibrational frequency scale factors. *J. Phys. Chem. A* **2007**, *111*, 11683–11700.
- (21) Clabo, D. A.; Allen, W. D.; Remington, R. B.; Yamaguchi, Y.; Schaefer, H. F., III. A systematic study of molecular vibrational anharmonicity and vibration–rotation interaction by self-consistent-field higher-derivative methods. Asymmetric top molecules. *Chem. Phys.* **1988**, *123*, 187–239.
- (22) Schneider, W.; Thiel, W. Anharmonic force fields from analytic second derivatives: Method and application to methyl bromide. *Chem. Phys. Lett.* **1989**, *157*, 367–373.
- (23) Barone, V. Anharmonic vibrational properties by a fully automated second-order perturbative approach. *J. Chem. Phys.* **2005**, *122*, 014108–014110.
- (24) Sibert, E. L. Variational and perturbative descriptions of highly vibrationally excited molecules. *Int. Rev. Phys. Chem.* **1990**, *9*, 1–27.
- (25) Christiansen, O. Møller–Plesset perturbation theory for vibrational wave functions. *J. Chem. Phys.* **2003**, *119*, 5773–5781.
- (26) Gaigeot, M. P. Theoretical spectroscopy of floppy peptides at room temperature. A DFTMD perspective: Gas and aqueous phase. *Phys. Chem. Chem. Phys.* **2010**, *12*, 3336–3359.
- (27) Bowman, J. M.; Christoffel, K.; Tobin, F. Application of SCF-SI theory to vibrational motion in polyatomic-molecules. *J. Phys. Chem.* **1979**, *83*, 905–912.
- (28) Thompson, T. C.; Truhlar, D. G. SCF CI calculations for vibrational eigenvalues and wavefunctions of systems exhibiting fermi resonance. *Chem. Phys. Lett.* **1980**, *75*, 87–90.
- (29) Ratner, M. A.; Buch, V.; Gerber, R. B. The semiclassical self-consistent-field (SC-SCF) approach to energy levels of coupled vibrational modes. II. The semiclassical state-interaction procedure. *Chem. Phys.* **1980**, *53*, 345.
- (30) Wang, X.-G.; Carrington, T., Jr. Six-dimensional variational calculation of the bending energy levels of HF trimer and DF trimer. *J. Chem. Phys.* **2001**, *115*, 9781–9796.
- (31) Avila, G.; Carrington, T., Jr. Nonproduct quadrature grids for solving the vibrational Schrödinger equation. *J. Chem. Phys.* **2009**, *131*, 174103–174115.
- (32) Avila, G.; Carrington, T., Jr. Solving the vibrational Schrödinger equation using bases pruned to include strongly coupled functions and compatible quadratures. *J. Chem. Phys.* **2012**, *137*, 174108–174113.
- (33) Bowman, J. M. Self-consistent field energies and wavefunctions for coupled oscillators. *J. Chem. Phys.* **1978**, *68*, 608–610.
- (34) Carney, G. D.; Sprandel, L. L.; Kern, C. W. Variational approaches to vibration–rotation spectroscopy for polyatomic molecules. *Adv. Chem. Phys.* **1978**, *37*, 305–379.
- (35) Cohen, M.; Greita, S.; McEarchran, R. D. Approximate and exact quantum mechanical energies and eigenfunctions for a system of coupled oscillators. *Chem. Phys. Lett.* **1979**, *60*, 445–450.
- (36) Gerber, R. B.; Ratner, M. A. Semi-classical self-consistent field (SC-SCF) approximation for eigenvalues of coupled-vibration systems. *Chem. Phys. Lett.* **1979**, *68*, 195–198.
- (37) Garrett, B. C.; Truhlar, D. G. Semiclassical self-consistent-field method for reactive resonances. *Chem. Phys. Lett.* **1982**, *92*, 64–70.
- (38) Roy, T. K.; Prasad, M. D. Effective harmonic oscillator description of anharmonic molecular vibrations. *J. Chem. Sci.* **2009**, *121*, 805–810.
- (39) Meng, K.; Wang, J. Anharmonic overtone and combination states of glycine and two model peptides examined by vibrational self-consistent field theory. *Phys. Chem. Chem. Phys.* **2011**, *13*, 2001–2013.

- (40) Roitberg, A.; Gerber, R. B.; Elber, R.; Ratner, M. A. Anharmonic wave-functions of proteins - Quantum self-consistent-field calculations of BPTI. *Science* **1995**, *268*, 1319–1322.
- (41) Roitberg, A. E.; Gerber, R. B.; Ratner, M. A. A vibrational eigenfunction of a protein: anharmonic coupled-mode ground and fundamental excited states of BPTI. *J. Phys. Chem. B* **1997**, *101*, 1700–1706.
- (42) Jung, J. O.; Gerber, R. B. Vibrational wave functions and spectroscopy of $(\text{H}_2\text{O})_n$, $n=2, 3, 4, 5$: Vibrational self-consistent field with correlation corrections. *J. Chem. Phys.* **1996**, *105*, 10332–10348.
- (43) Norris, L. S.; Ratner, M. A.; Roitberg, A. E.; Gerber, R. B. Møller–Plesset perturbation theory applied to vibrational problems. *J. Chem. Phys.* **1996**, *105*, 11261–11267.
- (44) Jung, J. O.; Gerber, R. B. Vibrational wave functions and energy levels of large anharmonic clusters: A vibrational SCF study of Ar_{13} . *J. Chem. Phys.* **1996**, *105*, 10682–10690.
- (45) Pele, L.; Brauer, B.; Gerber, R. B. Acceleration of correlation-corrected vibrational self-consistent field calculation times for large polyatomic molecules. *Theor. Chem. Acc.* **2007**, *117*, 69–72.
- (46) Pele, L.; Gerber, R. B. On the number of significant mode-mode anharmonic couplings in vibrational calculations: Correlation-corrected vibrational self-consistent field treatment of di-, tri-, and tetrapeptides. *J. Chem. Phys.* **2008**, *128*, 165105–165110.
- (47) Carter, S.; Bowman, J. M. The adiabatic rotation approximation for rovibrational energies of many-mode systems: Description and tests of the method. *J. Chem. Phys.* **1998**, *108*, 4397–4404.
- (48) Christoffel, K. M.; Bowman, J. M. Investigations of self-consistent field, SCF CI and virtual state configuration interaction vibrational energies for a model three-mode system. *Chem. Phys. Lett.* **1982**, *85*, 220–224.
- (49) Rauhut, G. Efficient calculation of potential energy surfaces for the generation of vibrational wave functions. *J. Chem. Phys.* **2004**, *121*, 9313–9322.
- (50) Bowman, J. M.; Carter, S.; Huang, X. C. MULTIMODE: A code to calculate rovibrational energies of polyatomic molecules. *Int. Rev. Phys. Chem.* **2003**, *22*, 533–549.
- (51) Carter, S.; Culik, S. J.; Bowman, J. M. Vibrational self-consistent field method for many-mode systems: A new approach and application to the vibrations of CO adsorbed on Cu(100). *J. Chem. Phys.* **1997**, *107*, 10458–10469.
- (52) Benoit, D. M. Fast vibrational self-consistent field calculations through a reduced mode-mode coupling scheme. *J. Chem. Phys.* **2004**, *120*, 562–573.
- (53) Scribano, Y.; Benoit, D. M. Calculation of vibrational frequencies through a variational reduced-coupling approach. *J. Chem. Phys.* **2007**, *127*, 164118–164118.
- (54) Yagi, K.; Hirata, S.; Hirao, K. Vibrational quasi-degenerate perturbation theory: applications to fermi resonance in CO_2 , H_2CO , and C_6H_6 . *Phys. Chem. Chem. Phys.* **2008**, *10*, 1781–1788.
- (55) Culot, F.; Lievin, J. A multiconfigurational SCF computational method for the resolution of the vibrational Schrödinger equation in polyatomic molecules. *Theor. Chem. Acc.* **1994**, *89*, 227–250.
- (56) Heislbez, S.; Rauhut, G. Vibrational multiconfiguration self-consistent field theory: Implementation and test calculations. *J. Chem. Phys.* **2010**, *132*, 124102–124107.
- (57) Roy, T. K.; Prasad, M. D. A thermal self-consistent field theory for the calculation of molecular vibrational partition functions. *J. Chem. Phys.* **2009**, *131*, 174102–174107.
- (58) Roy, T. K.; Prasad, M. D. Development of a new variational approach for thermal density matrices. *J. Chem. Phys.* **2011**, *134*, 214110–214118.
- (59) Keceli, M.; Hirata, S. Size-extensive vibrational self-consistent field method. *J. Chem. Phys.* **2011**, *135*, 134108–134111.
- (60) Hansen, M. B.; Christiansen, O.; Toffoli, D.; Kongsted, J. A virtual vibrational self-consistent-field method for efficient calculation of molecular vibrational partition functions and thermal effects on molecular properties. *J. Chem. Phys.* **2008**, *128*, 174106–174114.
- (61) Matsunaga, N.; Chaban, G. M.; Gerber, R. B. Degenerate perturbation theory corrections for the vibrational self-consistent field approximation: Method and applications. *J. Chem. Phys.* **2002**, *117*, 3541–3547.
- (62) Daněček, P.; Bouř, P. Comparison of the numerical stability of methods for anharmonic calculations of vibrational molecular energies. *J. Comput. Chem.* **2007**, *28*, 1617–1624.
- (63) Bloino, J.; Biczysko, M.; Barone, V. General perturbative approach for spectroscopy, thermodynamics, and kinetics: Methodological background and benchmark studies. *J. Chem. Theor. Comput.* **2012**, *8*, 1015–1036.
- (64) Heislbez, S.; Pfeiffer, F.; Rauhut, G. Configuration selection within vibrational multiconfiguration self-consistent field theory: Application to bridged lithium compounds. *J. Chem. Phys.* **2011**, *134*, 204108–204106.
- (65) Njagic, B.; Gordon, M. S. Exploring the effect of anharmonicity of molecular vibrations on thermodynamic properties. *J. Chem. Phys.* **2006**, *125*, 224102–224112.
- (66) Brauer, B.; Chaban, G. M.; Gerber, R. B. Spectroscopically-tested, improved, semi-empirical potentials for biological molecules: Calculations for glycine, alanine and proline. *Phys. Chem. Chem. Phys.* **2004**, *6*, 2543–2556.
- (67) Carter, S.; Bowman, J. M.; Harding, L. B. Ab initio calculations of force fields for H_2CN and ClHCN and vibrational energies of H_2CN . *Spectchim. Acta, Part A* **1997**, *53*, 1179–1188.
- (68) Roy, T. K.; Gerber, R. B. Vibrational self-consistent field calculations for spectroscopy of biological molecules: New algorithmic developments and applications. *Phys. Chem. Chem. Phys.* **2013**, *15*, 9468–9492.
- (69) Schmidt, M. W.; Baldridge, K. K.; Boatz, J. A.; Elbert, S. T.; Gordon, M. S.; Jensen, J. H.; Koseki, S.; Matsunaga, N.; Nguyen, K. A.; Su, S. J.; Windus, T. L.; Dupuis, M.; Montgomery, J. A. General atomic and molecular electronic-structure system. *J. Comput. Chem.* **1993**, *14*, 1347–1363.
- (70) Seidler, P.; Kongsted, J.; Christiansen, O. Calculation of vibrational infrared intensities and raman activities using explicit anharmonic wave functions. *J. Phys. Chem. A* **2007**, *111*, 11205–11213.
- (71) Pele, L.; Sebek, J.; Potma, E. O.; Gerber, R. B. Raman and IR spectra of butane: Anharmonic calculations and interpretation of room temperature spectra. *Chem. Phys. Lett.* **2011**, *515*, 7–12.
- (72) Dunning, T. H., Jr. Gaussian basis sets for use in correlated molecular calculations. I. The atoms boron through neon and hydrogen. *J. Chem. Phys.* **1989**, *90*, 1007–1023.
- (73) Miller, Y.; Chaban, G. M.; Gerber, R. B. Theoretical study of anharmonic vibrational spectra of HNO_3 , $\text{HNO}_3\text{-H}_2\text{O}$, HNO_4 : Fundamental, overtone and combination excitations. *Chem. Phys.* **2005**, *313*, 213–224.
- (74) Miller, B. J.; Soderfren, A. H.; Kjaeragaard, H. G. Vibrational overtone spectroscopy of three-membered rings. *J. Phys. Chem. A* **2007**, *111*, 5415–5421.
- (75) Miller, Y.; Chaban, G. M.; Gerber, R. B. Ab initio vibrational calculations for H_2SO_4 and $\text{H}_2\text{SO}_4\text{-H}_2\text{O}$: Spectroscopy and the nature of the anharmonic couplings. *J. Phys. Chem. A* **2005**, *109*, 6565–6574.
- (76) Stopperka, K.; Kitz, F. Z. Infrarotspektroskopische untersuchungen der gasphase über dem flüssigen system $\text{SO}_3\text{-H}_2\text{O}$. I. Die zusammensetzung der gasphase über dem flüssigen system $\text{H}_2\text{O-H}_2\text{SO}_4$ in abhängigkeit von der temperatur. *Anorg. Allg. Chem.* **1969**, *370*, 49–58.
- (77) Eng, R. S.; Petagana, G.; Nill, K. W. Ultrahigh (10^{-4} cm^{-1}) resolution study of the 8.2- μm and 11.3- μm bands of H_2SO_4 : Accurate determination of absorbance and dissociation constants. *Appl. Opt.* **1978**, *17*, 1723–1726.
- (78) Stepanian, S. G.; Reva, I. D.; Radchenko, E. D.; Rosado, M. T. S.; Duarte, M. L. T. S.; Fausto, R.; Adamowicz, L. Matrix-isolation infrared and theoretical studies of the glycine conformers. *J. Phys. Chem. A* **1998**, *102*, 1041–1052.
- (79) Godfrey, P. D.; Brown, R. D.; Rodgers, F. M. The missing conformers of glycine and alanine: Relaxation in seeded supersonic jets. *J. Mol. Struct.* **1996**, *376*, 65–81.

- (80) Chaban, G. M.; Jung, J. O.; Gerber, R. B. Anharmonic vibrational spectroscopy of glycine: Testing of ab initio and empirical potentials. *J. Phys. Chem. A* **2000**, *104*, 10035–10044.
- (81) Barone, V.; Biczysko, M.; Bloino, J.; Puzzarini, C. Glycine conformers: A never-ending story? *Phys. Chem. Chem. Phys.* **2012**, *15*, 1358–1363.
- (82) Stepanian, S. G.; Reva, I. D.; Radchenko, E. D.; Adamowicz, L. Conformational behavior of α -alanine. Matrix-isolation infrared and theoretical DFT and ab initio study. *J. Phys. Chem. A* **1998**, *102*, 4623–4629.
- (83) Reisner, D. E.; Field, R. W.; Kinsey, J. L.; Dai, H. L. Stimulated emission spectroscopy: A complete set of vibrational constants for X1A1 formaldehyde. *J. Chem. Phys.* **1984**, *80*, 5968–5978.
- (84) Frisch, M. J.; et al. *Gaussian 09*, revision A.02; Gaussian, Inc.: Wallingford, CT, 2009.
- (85) Fogarasi, G.; Zhou, X.; Taylor, P. W.; Pulay, P. The calculation of ab initio molecular geometries: Efficient optimization by natural redundant coordinates and empirical correction by offset forces. *J. Am. Chem. Soc.* **1992**, *114*, 8191–8201.
- (86) Horn, T. R.; Gerber, R. B.; Valentini, J. J.; Ratner, M. A. Vibrational states and structure of Ar₃: The role of three-body forces. *J. Chem. Phys.* **1991**, *94*, 6728–6736.
- (87) Horn, T. R.; Gerber, R. B.; Ratner, M. A. Vibrational states of very floppy clusters: Approximate separability and the choice of good curvilinear coordinates for XeHe₂, I₂He. *J. Chem. Phys.* **1989**, *91*, 1813–1823.
- (88) Bačič, Z.; Gerber, R. B.; Ratner, M. A. Vibrational levels and tunneling dynamics by the optimal coordinates, self-consistent field method: A Study of HCN \leftrightarrow HNC. *J. Phys. Chem.* **1986**, *90*, 7374–7381.
- (89) Thompson, T. C.; Truhlar, D. G. Optimization of vibrational coordinates, with an application to the water molecule. *J. Chem. Phys.* **1982**, *77*, 3031–3035.
- (90) Yagi, K.; Keceli, M.; Hirata, S. Optimized coordinates for anharmonic vibrational structure theories. *J. Chem. Phys.* **2012**, *137*, 204118–204116.
- (91) Njegic, B.; Gordon, M. S. Predicting accurate vibrational frequencies for highly anharmonic systems. *J. Chem. Phys.* **2008**, *129*, 164107–164113.
- (92) Suwan, I.; Gerber, R. B. VSCF in internal coordinates and the calculation of anharmonic torsional mode transitions. *Chem. Phys.* **2010**, *373*, 267–273.
- (93) Scribano, Y.; Lauvergnat, D. M.; Benoit, D. M. Fast vibrational configuration interaction using generalized curvilinear coordinates and self-consistent basis. *J. Chem. Phys.* **2010**, *133*, 094103–094112.